

# Simulating Interactions Between Coronal Mass Ejections

Damen Beverlin, Tatiana Niembro

## Abstract

Coronal mass ejections (CMEs) launch large amounts of plasma and magnetic fields into the interplanetary medium. Under the right initial conditions, this ejecta can reach Earth and cause issues with electronic devices. As such, we would like to have an accurate model that depicts how these CMEs propagate as they leave the sun. By using fluid dynamics and one-minute resolution in-situ solar wind data, we sought to simulate CME plasma propagation with analytical and numerical models. Because the interstellar medium contains other material and other events happen on the sun simultaneously, CMEs can interact with each other and other ejecta, which can cause them to change, so in order to have an accurate simulation we considered these interactions in our model. For our model, we made the assumption that the plasma was an ideal fluid, was super-alfvenic, and we employed an injection radius of  $10 R_{\odot}$ .

## I. Introduction

Coronal mass ejections (CMEs) are the largest and most energetic structures produced and expelled from the Sun, carrying large amounts of mass and strong magnetic fields (Zurbuchen & Richardson 2006 & Richardson and Cane, 2010). The arrival of the strongest and largest ones are the cause of auroras, as well as electrical disruptions and black outs that have cost millions of dollars. We model interactions between CMEs because they can cause changes in structure, increasing their strength and making them even more dangerous. From a theoretical point of view, both analytical (Borgazzi et al. 2009 and Vršnak et al. 2010, 2013) and numerical models (various models are reviewed by Zhao & Dryer 2014 and Lugaz et al. 2017) have been

developed to better understand how interplanetary coronal mass ejections (ICME) evolve and propagate while considering the possibility of interactions. Analytical models can predict the travel time, speed, and density of the ejecta at any heliospheric distance, but they cannot predict the in-situ time-profiles for conditions observed at 1 AU. Most numerical models have good predictions of the arrival magnitudes of the velocity and density of ICMEs, but the time-profile morphology of the in-situ parameters are relatively poor. Better prediction requires improvements in the uncertainties in the input parameters, knowledge of 3-D morphology and kinematics and the real background solar wind, and other known (deflection, reconnection, etc.) and unknown factors. In this work we focus on setting up the predictivity of variable solar wind conditions by simulating complex events. We do this by employing a combination of analytical and numerical models to create a 1-dimensional simulation of these events, with the goal of accurately predicting ICME evolution and propagation.

## II. Data

The events that we took into consideration come from the CME catalog that is generated and maintained at the Coordinated Data Analysis Web (CDAW) Data Center. The CME event that we chose as a sample occurred on May 28th, 2011. We used high-resolution data from the OMNIWeb service. The service was used to retrieve 1-minute resolution solar-wind data of our event, which was acquired from Advanced Composition Explorer (ACE), the Wind spacecraft, and Interplanetary Monitoring Platform (IMP). We looked at a 48-hour period of time from 12:00am May 27, 2011 to 12:00am May 29, 2011. The 1-minute resolution data was used to analyze the magnetic field magnitude ( $|B|$ ) and components ( $B_n$ ), the velocity magnitude ( $|V|$ ) and components ( $V_n$ ), the temperature ( $T$ ), the magnetic ( $P_{mag}$ ) and dynamic ( $P_{dyn}$ ) pressures, and the particle density ( $N$ ) of the solar wind as detected at Earth, or at 1 AU. We then utilized the

Disturbance Storm-Time (DST) index provided by the World Data Center (WDC) for Geomagnetism, Kyoto. We used 5-minute resolution disturbance storm time ( $D_{st}$ ) data for our event.

The purpose of utilizing this data was to confirm that the time-period that we chose contained traces of a CME event. The CME would have different values than the ambient solar wind, so we look for the following signs. If a CME was detected, we would expect that the temperature values would drop. The magnetic structure that accompanies the CME would cause an increase in the magnitude of the magnetic field, and resolved structure in the x, y, and z components may be visible. CMEs are likely to be faster than the ambient solar wind, so we look for increases in velocity magnitude, and we expect the plasma to be more dense, or have more particles per cubic centimeter (Kilpua 2017).

We plotted this data as shown on Figure 1. The first plot shows the  $|B|$  in black and  $T$  in red, each plotted on different axes. The second plot shows  $B_x$  in blue,  $B_y$  in green, and  $B_z$  in black, which allows us to look for resolved structure. The third plot shows  $V_x$  in blue on the left axis, and  $V_y$  in green and  $V_z$  in black on the right axis due to different directions and magnitudes. The fourth plot shows  $P_{dyn}$  and  $P_{mag}$  in nPa on different axes, which we use to see and compare the changes in the pressures of the plasma. The fifth plot shows the  $D_{st}$  over our time period, where a decrease in its value corresponds to interaction between the Earth and the solar wind's magnetic fields and we expect a CME to cause a large decrease. The sixth plot shows the particle density  $N$  and the seventh plot shows the  $|V|$  of the plasma, which we will use for our models.

We looked for markers of CME and interaction events and we marked these time periods on figure 1 with vertical black bars. The narrower time region is believed to show signs of interaction due to the spikes in the velocity and magnetic field of the solar wind, which would be

caused by a collision between two different solar wind objects such as two CMEs. The broader region is associated with a CME due to the drop in temperature, the structure in the components of the magnetic field and the increase in its magnitude, the increase in velocity, as well as the decrease in the  $D_{st}$ .

The models that we employ only require the density and velocity magnitude of the solar wind data at 1 AU. Originally we encountered difficulties with interpreting the results for the analytical model. Due to using 2,880 1-minute resolution data points, the model results were full of noise, so we chose to average the data to a 1-hour resolution. A comparison of the two can be seen in Figure 2, where the original data is plotted in green and our 1-hour average results are plotted in black.

### **III. Analytical Model**

Our analytical model allows us to take data gathered at 1 AU and find out its initial value at our injection radius of  $10 R_{\odot}$ . The model relies on a few assumptions about how we treat the plasma. We assume that the plasma is an ideal fluid so that we can use fluid dynamics to build up our model. We also claim that the plasma expands adiabatically, so that as it propagates, it accelerates. The other assumption that we make is that the plasma is super-alfvenic, meaning that it is moving faster than its characteristic Alfvén speed, or the speed of the propagation of the Alfvén wave through the plasma. Under this condition, the plasma is moving at a velocity such that the magnetic field that accompanies the CME does not have the ability to exert influence on the particles, which allows us to ignore the magnetic field. These assumptions are reasonable for our 1D model if we assume that the plasma detected occurs at or near the peak of the CME structure.

All of these assumptions allow us to employ Bernoulli's equations for fluid dynamics to derive initial conditions for our numerical model. The model uses our data values at 1 AU and solves for velocity ( $V_{inj}$ ) and density ( $N_{inj}$ ) of the plasma and the time ( $t_{inj}$ ) that it passes our injection radius. In order to make the model work, we have to make some assumptions and define constants. One constant is the heat capacity ratio (adiabatic index)  $\gamma$ , given as  $\gamma = (c_v+1)/c_v$ , where  $c_v$  is the heat capacity at constant volume and  $c_v = 1.5$  J/K for the plasma.  $T_{inj}$  is the temperature of the plasma at our injection radius, which we assume to be a constant  $10^5$  K due to its proximity to the Sun. We also have the molecular weight  $\mu$  of the plasma, which is  $\mu = 0.62$  or 62% as we assume that it has the same molecular abundance of the Sun (78% H, 28% He, 2% other).

We use Bernoulli's equation for velocity and modify it to take into consideration adiabatic expansion. We also make it so that our velocity is a ratio between  $V_{1AU}$  and  $V_{inj}$ . This leaves us with the equation:

$$V = \left(\frac{V_{1AU}}{V_{inj}}\right)^2 + \left(\frac{\gamma}{\gamma - 1}\right)\left(\frac{2k_b T_{inj}}{\mu m_p V_{inj}^2}\right)\left(\frac{r_{inj}}{R_{1AU}}\right)^{2(\gamma-1)}\left(\frac{V_{inj}}{V_{1AU}}\right)^{(\gamma-1)} - 1 - \left(\frac{\gamma}{\gamma - 1}\right)\left(\frac{2k_b T_{inj}}{\mu m_p V_{inj}^2}\right) \quad (1)$$

where  $m_p$  is the mass of a proton and  $k_b$  is the Boltzmann constant. We input our values for  $V_{1AU}$  and used the Python library SymPy to solve for  $V_{inj}$ .

In order to find the density of the plasma at our injection radius, we used Bernoulli's equation for mass-loss rate ( $\dot{m}_p$ ) to find the change in density, which we assume to be constant as it expands. We found our values by taking the equation:

$$\dot{m}_p = 4\pi\mu m_p R_{1AU}^2 N_{1AU} V_{1AU} \frac{(10^{15} \cdot 3.1536 \cdot 10^6)}{M_{\odot}} \quad (2)$$

and using Python to solve it for our values of  $N_{1AU}$  and  $V_{1AU}$ .

To utilize these values that are associated with a plasma, we need to know when these plasmas were present at our injection radius. We also wish to shift our time to be in terms of the injection radius ( $t_{inj}$ ) First we find the transit time ( $T_T$ ) of our plasma by taking its velocity  $V_{1AU}$ , assume it was constant as it travels 1 AU, and subtract that time from  $t_{1AU}$ :

$$T_T = t_{1AU} - \frac{R_{1AU}}{V_{1AU}} \quad (3)$$

Once we calculated this, we then find the time  $t_{inj}$  using  $V_{inj}$  and the distance between our injection radius and 1 AU:

$$t_{inj} = \frac{R_{1AU} - r_{inj}}{V_{inj}} \quad (4)$$

And then we can switch between these time frames with the equation:

$$t_{1AU} = t_{inj} + \Delta t \quad (5)$$

After solving for these values, we plotted  $V_{inj}$  and  $\dot{m}_p$  in terms of  $t_{inj}$ . These data points allow us to look for the initial plasma conditions of the various solar wind plasmas emitted from various events. In this data we look for plateau regions in our plot which show constant values of density and velocity. We associate these constant regions with an event, assuming that each event emits a plasma with a uniform density and velocity. Our results can be seen in figure 3, where the black dots represent the values we found, the blue lines show the order of these data points in terms of  $t_{1AU}$ , the colored regions show the time periods that we associated with a specific plasma, and the horizontal black lines show the average values of  $V_{inj}$  and  $\dot{m}_p$  for each plasma. The sections of the plots that do not fit in a plateau and overlap are the result of some of the assumptions that we make in our model. These regions are artifacts of missing time, which is addressed in the Results section.

## IV. Numerical Model

The numerical model takes the initial conditions that we found with the analytical model, and uses them to simulate the propagation of the plasma as it travels from  $r_{inj}$  to 1 AU. To do this, we define several solar wind plasmas using the  $V_{inj}$  and  $\dot{m}_p$  for each of our plasmas. The model calculates the pressure ( $P_{wind}$ ), density ( $N_{wind}$ ), and velocity ( $V_{wind}$ ) of each input plasma over 2,000 15-minute time steps from  $10 R_{\odot}$  to 1.2 AU. Each time step is simulated and recorded on one of the 1,200 pixels, where each pixel represents about 0.001 AU. In order to calculate these values, we employ well-known conservative equations. We use the following equation to find the density for each plasma at increasing distances from  $r_{inj}$ :

$$N_{wind} = \frac{M_{\odot}}{4\pi V_{wind} r^2} \quad (6)$$

where  $N_{wind}$  is the density at  $r$ ,  $V_{wind}$  is the velocity of the plasma,  $M_{\odot}$  is the mass of the plasma given from the product of its initial density and  $m_p$ , and  $r$  is the distance from  $r_{inj}$ .

Next we used the equation for momentum:

$$p_{wind} = N_{wind} V_{wind} \quad (7)$$

where  $p_{wind}$  is the momentum of the plasma, to find the momentum of the plasma at a given distance  $r$ .

We then use the equation for energy:

$$U_{wind} = 0.5 N_{wind} V_{wind}^2 + c_v P_{wind} \quad (8)$$

where  $P_{wind}$  is the dynamic pressure of the plasma and is found from the equation:

$$P_{wind} = \frac{p_{wind} R_g T_{inj}}{\mu} \quad (9)$$

where we assume that the temperature is constantly  $T_{inj}$ .

The model is operated using Fortran. In order to run it, all we have to do is define our constants and plug in the initial conditions for plasmas in chronological order and specify what distances we want the  $P_{\text{wind}}$ ,  $N_{\text{wind}}$ , and  $V_{\text{wind}}$  time-profiles to be calculated for (pick which pixels to return). The program is run through a shell, which returns a table that provides the time-step and the associated  $P_{\text{wind}}$ ,  $N_{\text{wind}}$ , and  $V_{\text{wind}}$  values detected at the specified distance.

The initial time-profiles for 1 AU can be seen in figure 4. This figure shows the results for the entire run-time of the simulation (500 hours). The first plot shows the  $P_{\text{wind}}$  time-profile, the second plot shows the  $N_{\text{wind}}$  time-profile, and the third plot shows the  $V_{\text{wind}}$  time-profile. The pressure time-profile has a black line and a red line. When we start our simulation we assume that the first plasma, the red section in figure 3, is the ambient solar wind, and we allow it to fill up the entire simulation space before we allow the other plasmas to permeate. We do this because we do not want the simulation to run in a vacuum, as that would affect the expansion of our plasma, and is not a realistic representation of the interplanetary medium. The red line represents the entire time-profile, but the black line represents the portion of the profile where the simulation has been filled and is usable.

The model can also be used to look at the time-profiles of the plasmas at various distances of travel. By looking at the results of individual pixels, we can see how the plasmas evolve as they interact with each other, as shown in figure 5. Each plot in figure 5 shows the  $N_{\text{wind}}$  time-profile (in blue) and  $V_{\text{wind}}$  time-profile (in black) for the corresponding distances given on the left axis. In the initial plot for 0.1 AU, we can see that the plateau-like initial conditions of the plasmas are still very apparent, but we also see peaks starting to form in-between them, which are the result of interactions between two plasmas. As we look at the results for further

and further distances, we see that the plateaus disappear more and more, and even the peaks begin to overlap. This shows that the initial plasmas are interacting with each other and evolving.

## V. Results

In order to compare our results for  $V_{IAU}$  and  $N_{IAU}$  that we achieved from our model to the actual value from the OMNI data, we need to make some adjustments. The first thing that we must do is that we must address the concern of missing time from our analytical model. Because our model takes advantage of many simplifications and assumptions, we do not consider many known and unknown factors that influence the propagation and interactions of these plasmas, such as momentum transfer between interacting plasmas. Due to these factors that are not considered, our model is not able to account for all of the time that our plasma propagates for, leading to periods of time that are not recognized by our model. In order to account for this missing time, we manually find the time between the data points in each of the overlapping regions of the analytical model results and add them to the time in our numerical model.

The addition of this missing time contributes to the 48-hour time period that we expect to get from our model. Once we make this correction, we then use our transit times from the analytical model and apply them to our numerical model results to align the starting times of the model and the data. The corrected results are then trimmed so that they focus on the 48-hour time window that we used for our OMNI data. Once all of this is done, we plot the 1-minute data, 1-hour data, and model results, on the same plot so that we can compare the accuracy of the results to the original data and the averaged data that we used to derive it.

The final results for our simulation can be seen in figure 6. The top plot shows the original velocity data as the black line, the 1-hour average as the green line, and the results of our simulation as the blue dotted line. The bottom plot shows the same thing but for the particle

density instead. Looking at the  $V$  plot, we can see that our model produced a  $V_{1AU}$  time-profile that matches the 1-hour average fairly well, but is not in great agreement with the original data, but we expect this. Looking at the  $N$  plot, we can see that our model fits neither the 1-hour average nor the original data very well. We achieved a similar morphology to the data, but the locations of peaks and troughs do not line up so well, and there is both overestimation and underestimation in density values. We believe that these discrepancies in our final results are caused by several issues with the approach that we took. Of course the same missing features that account for the missing time may contribute. We also believe that the use of a smaller average, such as 30 minutes, would keep more of the features of the original data and provide simulations with more accurate results.

## VI. Conclusions

We set out to make a 1D model that could simulate the propagation and interactions of a CME in the interplanetary medium. We chose a CME that was detected reaching Earth on May 28th, 2011 as our sample. We took 1-minute OMNI data for May 27th to May 29th, and examined it to make sure we know what we are looking at and what part of the data relates to the CME (figure 1). Once we understood this, we took the  $N_{1AU}$  and  $V_{1AU}$  from our data and averaged it to 1-hour resolution so that it is easier to work with (figure 2).

These values are then plugged into our analytical model, which employs Bernoulli's equations to solve for the value of the density ( $N_{inj}$ ) and velocity ( $V_{inj}$ ) of the plasma at our injection radius. We plot these values and look for plateau-like regions of constant  $N_{inj}$  and  $V_{inj}$  and associate them with a plasma, although our model leaves some missing time (figure 3). We take these plasmas as initial conditions for our numerical model, which uses conservative equations to create time-profiles of the  $P_{wind}$ ,  $N_{wind}$ , and  $V_{wind}$  of our plasmas at distances from the

Sun between  $r_{inj}$  and 1.2 AU. In order to compare the result of our model's timelines for 1 AU (figure 4) to our data, we need to make corrections to account for the missing time, and align the start times and trim the simulation results. Once we make our corrections we can compare the 1-minute data, 1-hour average, and simulation results (figure 6). We can also use the model to look at time-profiles for other distances to see how our plasmas are changing as they interact (figure 5).

The final results of our model show that there is still room for improvement. Due to the assumptions that we make for our 1D model, some factors that affect the propagation of CMEs and solar wind are not accounted for. In order to greatly improve our results, we need to understand what effects that our model is not considering. The model then needs to be modified so that it automatically considers the effects that are not modeled by our conservative equations and account for missing time. Another consideration to improve the results of our model is to use a finer average data size, such as a 30 minute data average, so that more of the features of the original data are resolved.

There is still more work to be done to test and improve the model. The results of the analytical model can be compared to remote sensing data for  $10 R_{\odot}$ . We would use side-profile images and data of our CME from the STEREO A and STEREO B instruments to compare our calculated  $V_{inj}$  and  $N_{inj}$  to measured values and test their accuracy. After improving the model to where the time-profiles it produces for 1 AU match the data sufficiently well, it can then be applied to other CME events of varying strengths and complexity to test how generally it can be used and provide accurate simulations. Once the 1D model is deemed sufficiently viable, we could then compare our work to other models that use different techniques and assumptions. The

next steps would also be to develop the model for 2D and 3D simulations so that it can provide results that are comparable to real-life CMEs.

### **Acknowledgements**

This work was supported by the NSF-REU solar physics program at SAO, grant number AGS-1850750. We would like to thank the CfA-REU organizers in particular Kathy Reeves and Chad Madsen. We acknowledge use of NASA/GSFC's Space Physics Data Facility's OMNIWeb (or CDAWeb or ftp) service, and OMNI data. This CME catalog is generated and maintained at the CDAW Data Center by NASA and The Catholic University of America in cooperation with the Naval Research Laboratory. SOHO is a project of international cooperation between ESA and NASA. The DST (Disturbance Storm-Time) index used in this paper was provided by the WDC for Geomagnetism, Kyoto.

### **Citations**

- Borgazzi, A., Lara, A., Echer, E., & Alves, M. V. (2009). Dynamics of coronal mass ejections in the interplanetary medium. *Astronomy and Astrophysics*, 498(3), 885-889.  
<https://doi.org/10.1051/0004-6361/200811171>
- Kilpua, E., Koskinen, H. E. J., & Pulkkinen, T. I. (2017). Coronal mass ejections and their sheath regions in interplanetary space. *Living Reviews in Solar Physics*, 14(1), 83.  
<https://doi.org/10.1007/s41116-017-0009-6>
- Lugaz, N., Temmer, M., Wang, Y., & Farrugia, C. J. (2017). The Interaction of Successive Coronal Mass Ejections: A Review. *Solar Physics*, 292(4), 37.  
<https://doi.org/10.1007/s11207-017-1091-6>

- Papitashvili, Natalia E. and King, Joseph H. (2020), "OMNI 1-min Data" [Data set], NASA Space Physics Data Facility, <https://doi.org/10.48322/45bb-8792>, Accessed on (06/11/2021)
- Papitashvili, Natalia E. and King, Joseph H. (2020), "OMNI 5-min Data" [Data set], NASA Space Physics Data Facility, <https://doi.org/10.48322/gbpg-5r77>, Accessed on (06/11/2021)
- Richardson, I. G., & Cane, H. V. (2010). Near-Earth Interplanetary Coronal Mass Ejections During Solar Cycle 23 (1996 - 2009): Catalog and Summary of Properties. *Solar Physics*, 264(1), 189-237. <https://doi.org/10.1007/s11207-010-9568-6>
- Vršnak, B., Žic, T., Falkenberg, T. V., Möstl, C., Vennerstrom, S., & Vrbanec, D. (2010). The role of aerodynamic drag in propagation of interplanetary coronal mass ejections. *Astronomy and Astrophysics*, 512(2010), A43. <https://doi.org/10.1051/0004-6361/200913482>
- Vršnak, B., Žic, T., Vrbanec, D., Temmer, M., Rollett, T., Möstl, C., Veronig, A., Čalogović, J., Dumbović, M., Lulić, S., Moon, Y. J., & Shanmugaraju, A. (2013). Propagation of Interplanetary Coronal Mass Ejections: The Drag-Based Model. *Solar Physics*, 285(1-2), 395-315. <https://doi.org/10.1007/s11207-012-0035-4>
- Zhao, X., & Dryer, M. (2014). Current status of CME/shock arrival time prediction. *Space Weather*, 12(7), 448-469. <https://doi.org/10.1002/2014SW001060>
- Zurbuchen, T. H., & Richardson, I. G. (2006). In-Situ Solar Wind and Magnetic Field Signatures of Interplanetary Coronal Mass Ejections. *Space Science Reviews*, 123(1-3), 31-43. <https://doi.org/10.1007/s11214-006-9010-4>

## Appendix

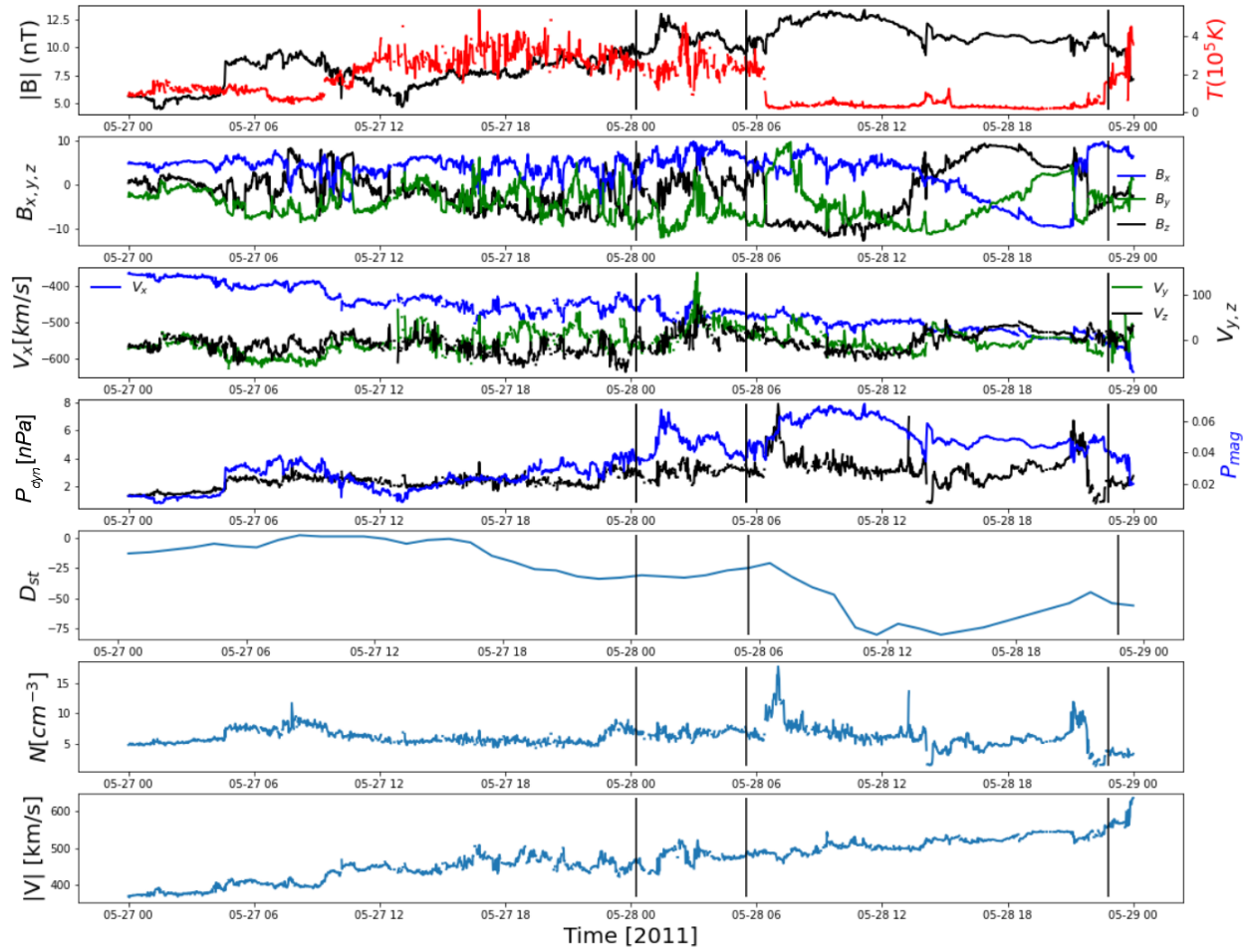


FIGURE 1. Solar wind data for the event of May 28th, 2011 from OMNI. The CME is reported in Wind ICME list as a flux-rope with its boundaries delimited by the two latter vertical lines.

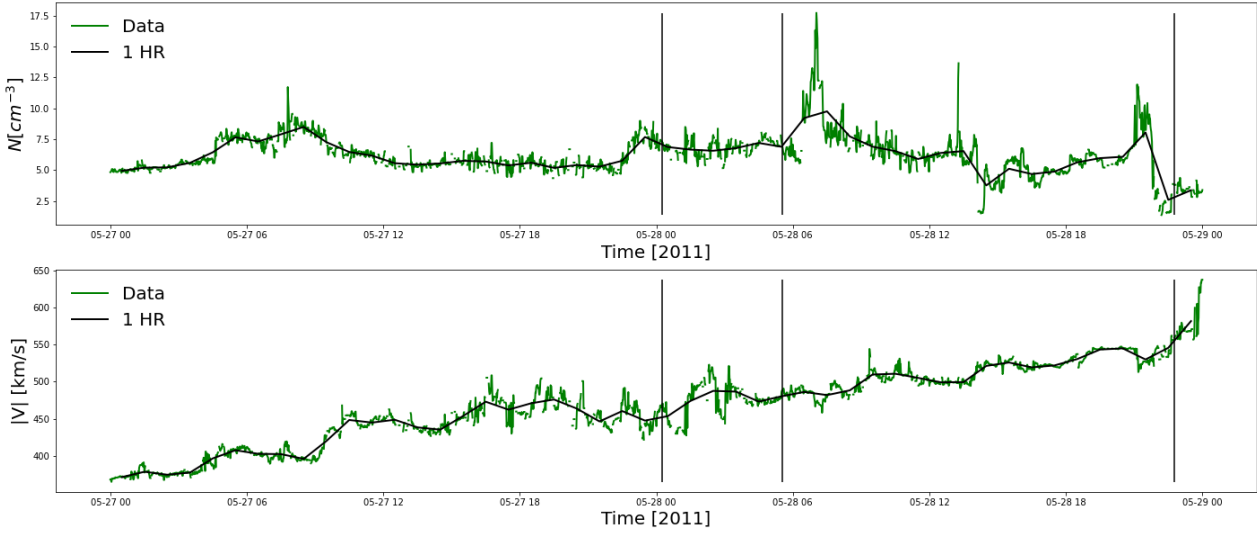


FIGURE 2. Comparison of the 1-minute resolution OMNI data  $N_{IAU}$  and  $V_{IAU}$  (green) to the 1-hour average  $N_{IAU}$  and  $V_{IAU}$  (black).

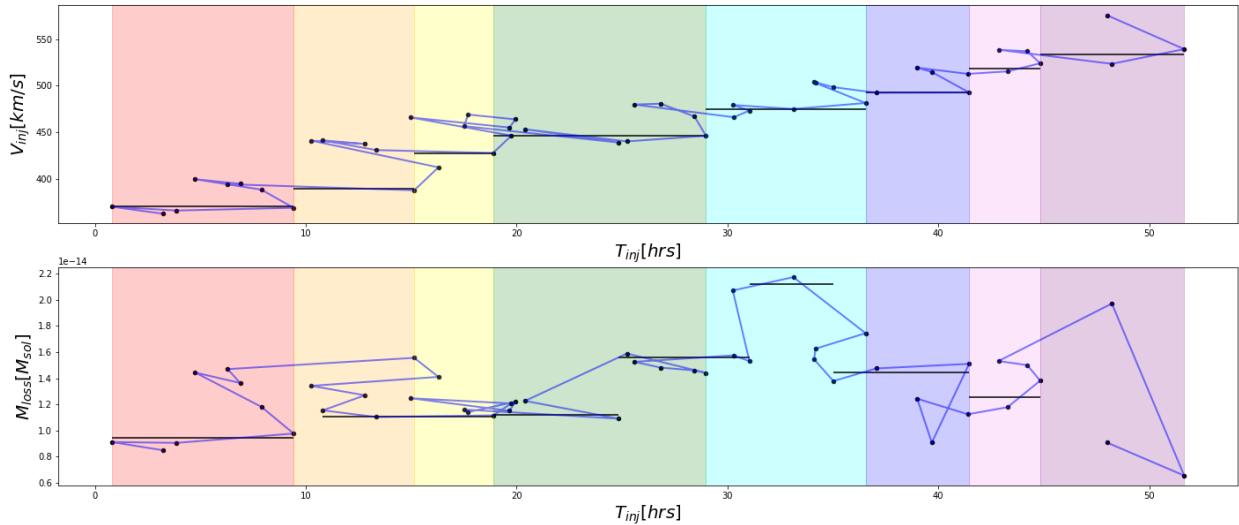


FIGURE 3. Reconstruction of the solar wind conditions expected at  $10 R_{\odot}$ . This is created from plugging in our data into the analytical model, which utilizes Bernoulli's equations. The equations predict the constant patches of plasma. The points outside of these patches account for missing time and are related to the interactions and cannot be modeled by the conservative equations.

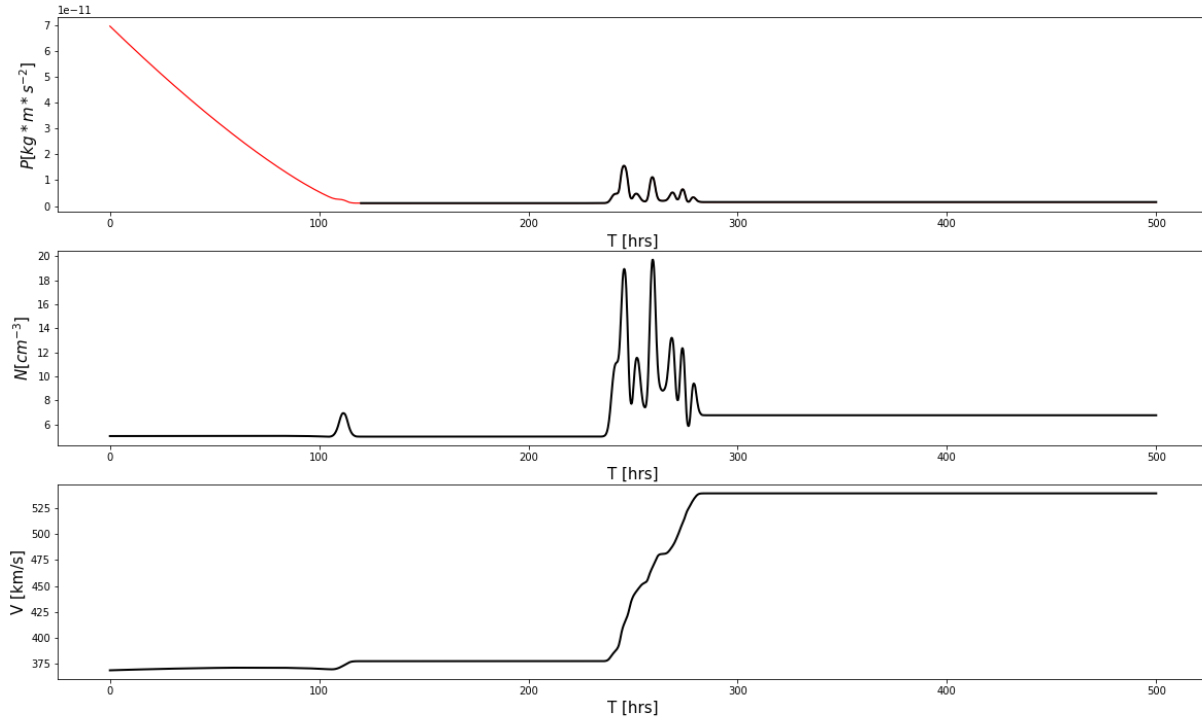


FIGURE 4. Results for  $P_{\text{wind}}$ ,  $N_{\text{wind}}$ , and  $V_{\text{wind}}$  from our numerical model at 1 AU. The portion of the  $P_{\text{wind}}$  plot denoted by the red line illustrates the time that it takes for our initial plasma to permeate our model so that the simulation does not operate in a vacuum. The black line on that plot denotes the time period of the simulation that we consider. On the  $N_{\text{wind}}$  and  $V_{\text{wind}}$  plots there is a bump around where the black line begins, which denotes the detection of the initial plasma at 1 AU.

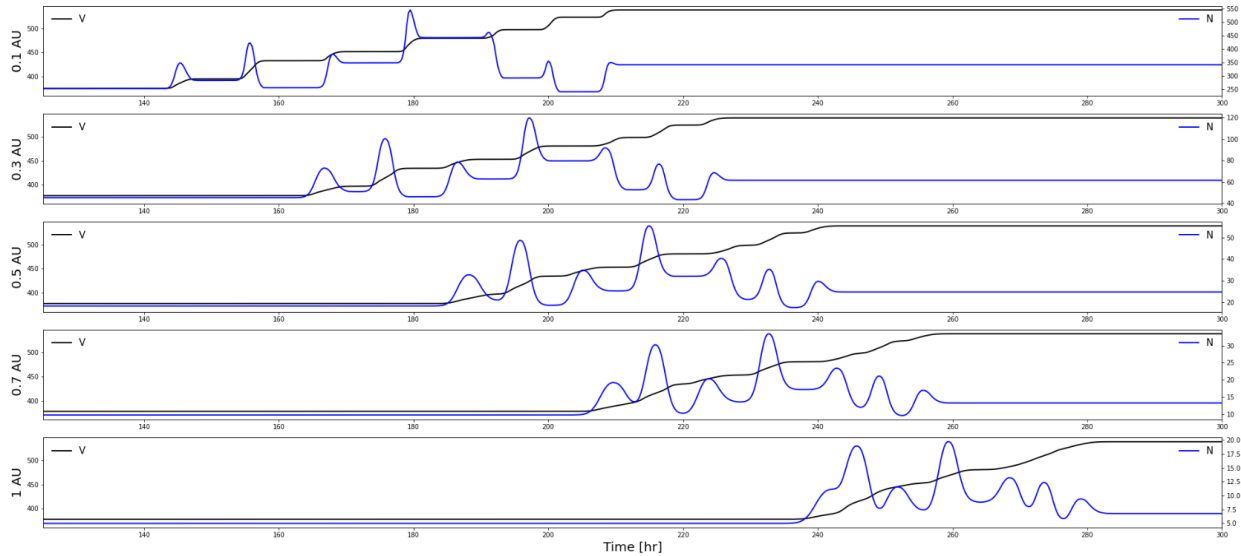


FIGURE 5. Results for  $N_{wind}$  and  $V_{wind}$  of pixels at given distances. The model assumes that the gas is blown away from the Sun at constant  $N_{wind}$ , and  $V_{wind}$ . Then, the conditions change for specific intervals of time (computed from the analytical reconstruction) by changing the original values by a constant factor. The difference in speed between patches will form compression regions and rarefactions. Compression regions are formed due to the interaction between different patches of plasma.

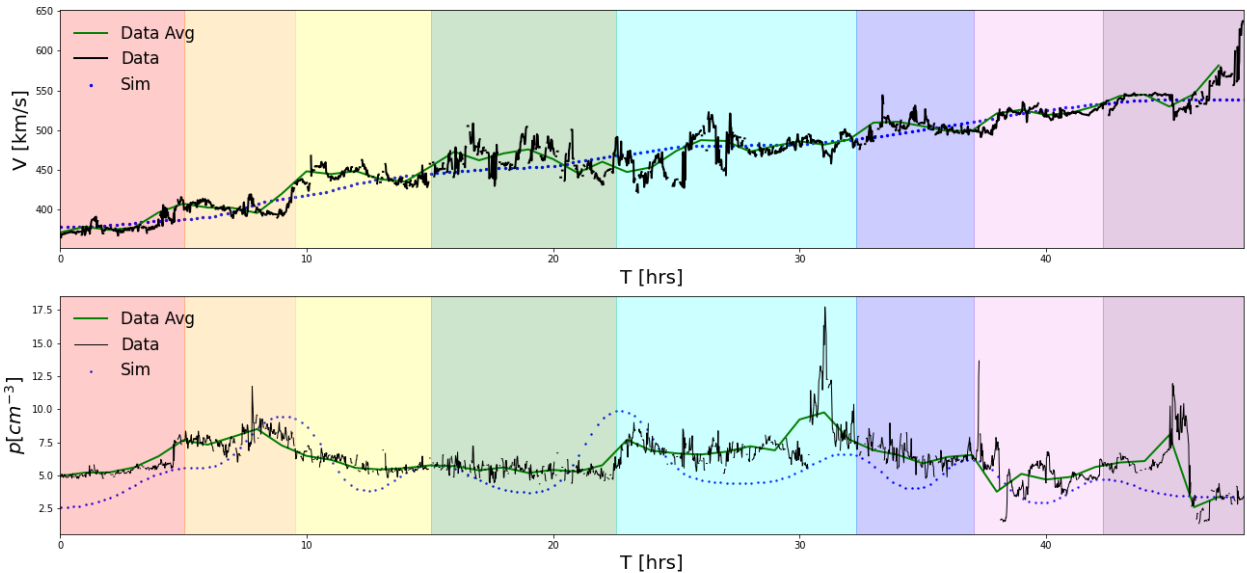


FIGURE 6. Time series of  $V_{1AU}$  and  $N_{1AU}$ . Colored regions correspond with plasmas of the model. The results of numerical simulations are shown in blue compared to one-minute (black) and one-hour (green) data.